



AFRL-AFOSR-VA-TR-2020-0153

---

**Plasmonic Amplification through On-Chip, Four-Wave Mixing in Hybrid 2D Material Plasmonic Structures**

**John Schaibley  
UNIVERSITY OF ARIZONA**

---

**06/26/2020  
Final Report**

DISTRIBUTION A: Distribution approved for public release.

Air Force Research Laboratory  
AF Office Of Scientific Research (AFOSR)/ RTB1  
Arlington, Virginia 22203  
Air Force Materiel Command

<b>REPORT DOCUMENTATION PAGE</b>				<i>Form Approved</i> OMB No. 0704-0188	
<p>The public reporting burden for this collection of information is estimated to average 1 hour per response, including the time for reviewing instructions, searching existing data sources, gathering and maintaining the data needed, and completing and reviewing the collection of information. Send comments regarding this burden estimate or any other aspect of this collection of information, including suggestions for reducing the burden, to Department of Defense, Executive Services, Directorate (0704-0188). Respondents should be aware that notwithstanding any other provision of law, no person shall be subject to any penalty for failing to comply with a collection of information if it does not display a currently valid OMB control number.</p> <p><b>PLEASE DO NOT RETURN YOUR FORM TO THE ABOVE ORGANIZATION.</b></p>					
<b>1. REPORT DATE (DD-MM-YYYY)</b> 01-09-2020		<b>2. REPORT TYPE</b> Final Performance		<b>3. DATES COVERED (From - To)</b> 01 Apr 2017 to 31 Mar 2020	
<b>4. TITLE AND SUBTITLE</b> Plasmonic Amplification through On-Chip, Four-Wave Mixing in Hybrid 2D Material Plasmonic Structures				<b>5a. CONTRACT NUMBER</b>	
				<b>5b. GRANT NUMBER</b> FA9550-17-1-0215	
				<b>5c. PROGRAM ELEMENT NUMBER</b> 61102F	
<b>6. AUTHOR(S)</b> John Schaibley				<b>5d. PROJECT NUMBER</b>	
				<b>5e. TASK NUMBER</b>	
				<b>5f. WORK UNIT NUMBER</b>	
<b>7. PERFORMING ORGANIZATION NAME(S) AND ADDRESS(ES)</b> UNIVERSITY OF ARIZONA 888 N EUCLID AVE RM 510 TUCSON, AZ 85719-4824 US				<b>8. PERFORMING ORGANIZATION REPORT NUMBER</b>	
<b>9. SPONSORING/MONITORING AGENCY NAME(S) AND ADDRESS(ES)</b> AF Office of Scientific Research 875 N. Randolph St. Room 3112 Arlington, VA 22203				<b>10. SPONSOR/MONITOR'S ACRONYM(S)</b> AFRL/AFOSR RTB1	
				<b>11. SPONSOR/MONITOR'S REPORT NUMBER(S)</b> AFRL-AFOSR-VA-TR-2020-0153	
<b>12. DISTRIBUTION/AVAILABILITY STATEMENT</b> A DISTRIBUTION UNLIMITED: PB Public Release					
<b>13. SUPPLEMENTARY NOTES</b>					
<b>14. ABSTRACT</b> We published the paper '2D Semiconductor Nonlinear Plasmonic Modulators' in Nature Communications in which we demonstrate ultra fast (290 fs) plasmonic modulation with low (~100 fJ) switching energies. We fabricated novel 2D material cross-propagating plasmonic structures that show a 175% differential transmission response. We are currently preparing a manuscript on our new results.					
<b>15. SUBJECT TERMS</b> nonlinear, Four-Wave Mixing, plasmonics, nonlinear plasmonic effects, plasmonic amplifiers, two-dimensional materials, 2D materials					
<b>16. SECURITY CLASSIFICATION OF:</b>			<b>17. LIMITATION OF ABSTRACT</b>  UU	<b>18. NUMBER OF PAGES</b>	<b>19a. NAME OF RESPONSIBLE PERSON</b> POMRENKE, GERNOT
<b>a. REPORT</b>  Unclassified	<b>b. ABSTRACT</b>  Unclassified	<b>c. THIS PAGE</b>  Unclassified			<b>19b. TELEPHONE NUMBER (Include area code)</b> 703-696-8426

**AFOSR Grant:** FA9550-17-1-0215

**PI:** John Schaibley, University of Arizona, Department of Physics

**Title:** Plasmonic Amplification through On-Chip, Four-Wave Mixing in Hybrid 2D Material Plasmonic Structures

**Final Report- June 2020**

### **Summary:**

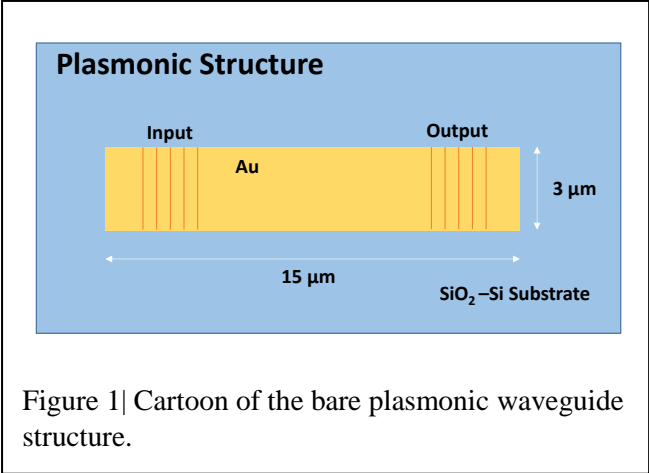
The overarching goal of this research is to develop novel 2D material plasmonic structures that can control and amplify surface plasmon polaritons (SPPs). SPPs are hybrid light-charge oscillations that propagate at metal surfaces and have applications to high speed optical information processing. During this AFOSR-YIP project, we successfully developed 2D material plasmonic structures, and demonstrated the first 2D semiconductor nonlinear plasmonic modulator with the potential to realize ultra-high speed ( $\sim 290$  fs) switching times with low ( $\sim 100$  fJ) switching energies. This was achieved by mechanically transferring single atomically thin WSe<sub>2</sub> monolayers on top of gold plasmonic waveguides and measuring the modulators linear and nonlinear transmission properties. The key to our architecture is the strong resonant nonlinear response of excitons (electron-hole pairs) bound to atomically thin transition metal dichalcogenide semiconductors. This work “2D Semiconductor Nonlinear Plasmonic Modulators” was published in Nature Communications in 2019. During the last year of the award, we developed “cross” waveguide structures allowing for the amplification of SPP waves, and are currently preparing a manuscript for publication. In addition, we filed a provisional patent entitled “Plasmonic Amplification through Nonlinear Wave Mixing in Hybrid Nonlinear Material Plasmonic Structures” on this concept. Our future projects are focused on building upon these successes to realize stronger nonlinear response through waveguide design and faster nonlinear response through 2D material heterostructures.

**Project Background:** The objectives of this project are to: 1) develop novel 2D material-plasmonic structures, 2) investigate their fundamental physical behavior and 3) demonstrate amplification of surface plasmon polaritons (SPPs) in hybrid 2D material/plasmonic structures using coherent wave mixing effects. SPPs comprise a free charge oscillation in a conductor (plasmon) coupled to the electromagnetic field (photon). SPPs allow for sub-free-space wavelength confinement of optical frequency waves for applications to ultra-high speed information processing. In this project, integrated 2D material layers (transition metal dichalcogenide, TMD) semiconductors serve as active elements, where the large third-order nonlinear susceptibility is used to control SPP amplitude. In addition, intrinsic SPPs confined to graphene and doped TMDs are to be investigated through nonlinear plasmonic spectroscopy.

### **Year 1 Results:**

*Metallic waveguide modelling and fabrication*

Metallic plasmonic waveguides were successfully designed, and optimized using a commercial software package (Lumerical). The waveguides comprise a 200 nm thick gold film. The waveguides have integrated diffraction grating couplers (five etched grooves) that are optimized for a transmission bandwidth of 40 nm around the WSe<sub>2</sub> exciton resonances (712 nm). A cartoon of the modeled device is shown in Figure 1, where Figure 2a shows the electric field profile midway through the waveguide, and Figure 2b shows the theoretical transmission curve for a focused Gaussian beam at normal incidence on the input grating coupler. The theoretical throughput of the device (free space input to free space output) is ~5% at 710 nm.



The rectangular metallic waveguides were fabricated via electron beam lithography followed by thermal evaporation of gold film. The grating couplers were etched into the rectangular waveguides by argon ion milling following a second lithography pattern. Figure 3 shows an AFM image of the grating couplers of the completed plasmonic waveguide. Figure 5a shows the experimentally measured transmission spectrum which is in good agreement with theory (Figure 2b).

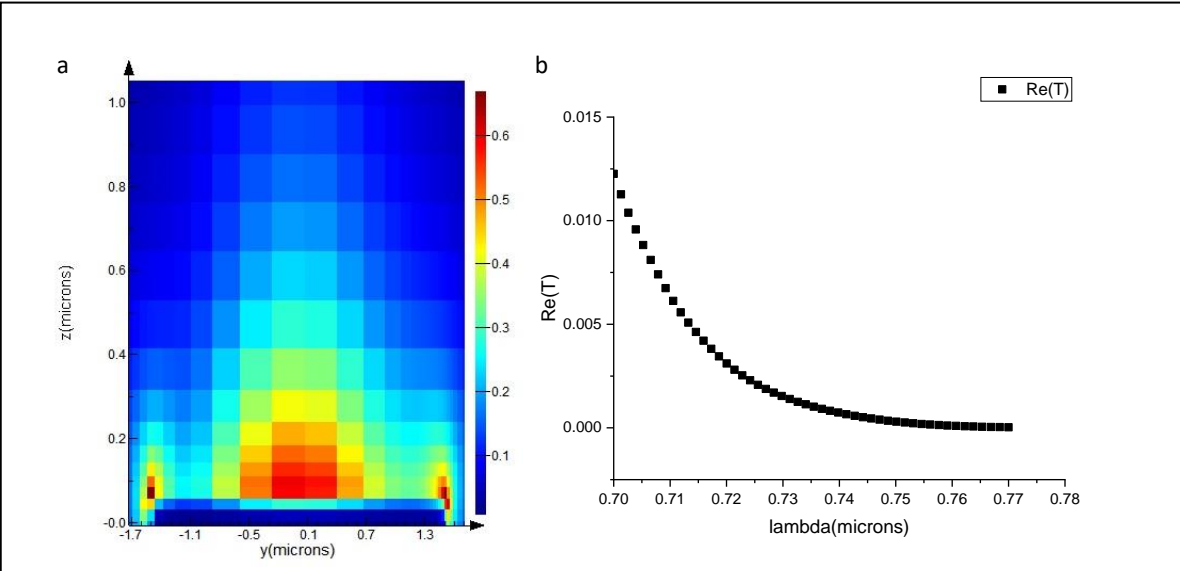


Figure 2| Lumerical simulations of the waveguide. a) Simulated electric field mode profile midway through the plasmonic waveguide. The color axis is in terms of the fraction of the incident electric field. b) The theoretical transmission spectrum of the plasmonic waveguide shown in Figure 1.

*Integration of 2D semiconductor layers onto metallic waveguides*

In this project, 2D semiconductor layers serve as the nonlinear element. In order to achieve this, monolayer WSe<sub>2</sub> must be integrated on top of the metallic waveguide structures. Monolayer WSe<sub>2</sub> was obtained through mechanical exfoliation from bulk crystals. In order to electrically isolate the WSe<sub>2</sub> from the metallic waveguide (to avoid quenching of excitons), it was encapsulated with ~10 nm thick 2D material insulator (hexagonal boron nitride, hBN). The hBN-WSe<sub>2</sub>-hBN heterostructure was transferred onto the prefabricated metallic waveguide structure (see description above) using a polymer based dry transfer technique (polycarbonate film on PDMS stamp). The alignment was carried out under a microscope allowing for sub-micron alignment of the 2D heterostructure to the center of the waveguide. An optical image of the resulting hybrid 2D material plasmonic structure is shown in Figure 4a.

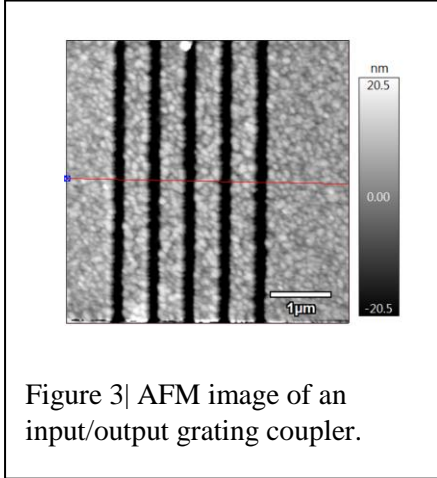


Figure 3| AFM image of an input/output grating coupler.

*Demonstration of coupling between SPPs and WSe<sub>2</sub> excitons*

The hybrid hBN-WSe<sub>2</sub>-hBN/plasmonic structure was investigated optically at 4 K in closed-cycle optical cryostat. A narrow bandwidth tunable laser was focused to a diffraction limited beam stop on the input grating. The light scattered out of the output coupler was isolated using spatial filtering and detected with an amplified silicon photodiode. The transmission spectrum is shown in Figure 5a. The cyan data show the transmission spectrum the hybrid hBN-WSe<sub>2</sub>-hBN/plasmonic structure, and the black show a reference bare waveguide. At the exciton resonance (712 nm), the transmission is reduced by approximately 50% due to the presence of the WSe<sub>2</sub> layer, indicating very strong coupling between SPPs and WSe<sub>2</sub> excitons. By comparing these

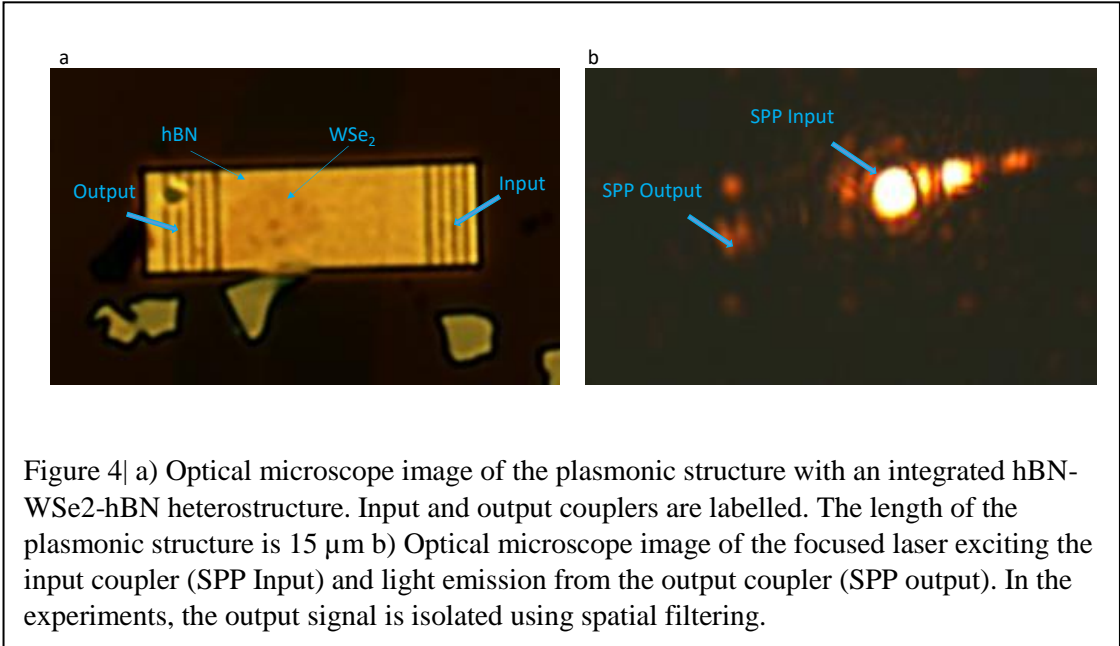
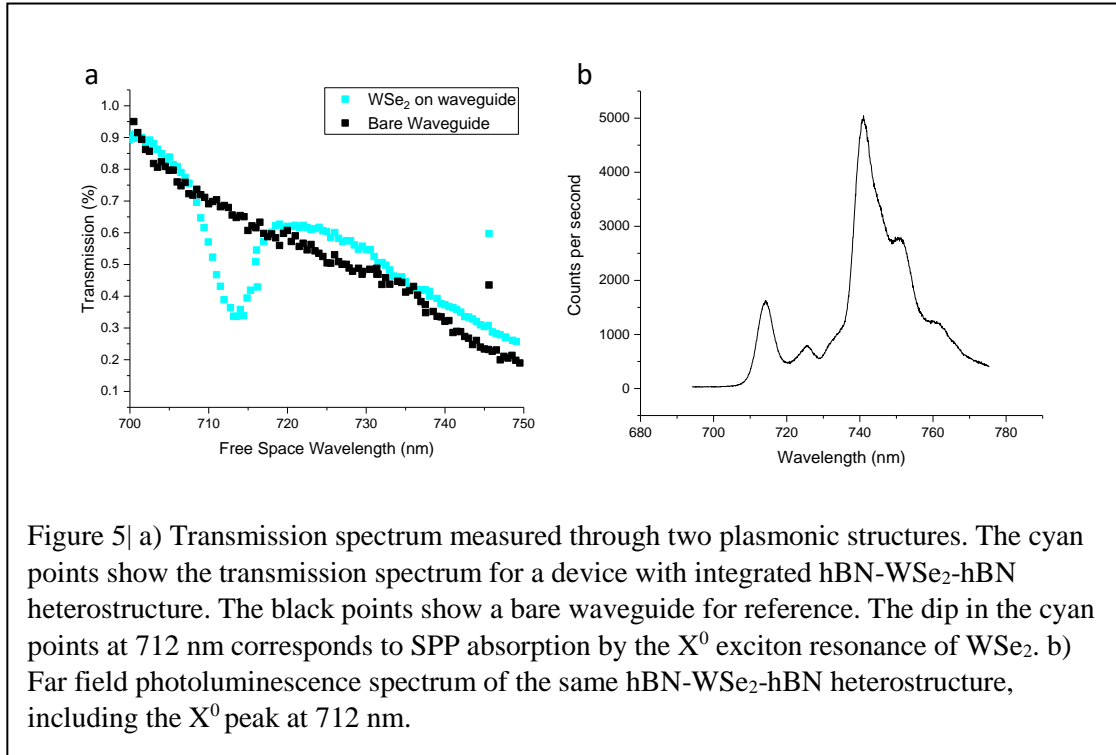
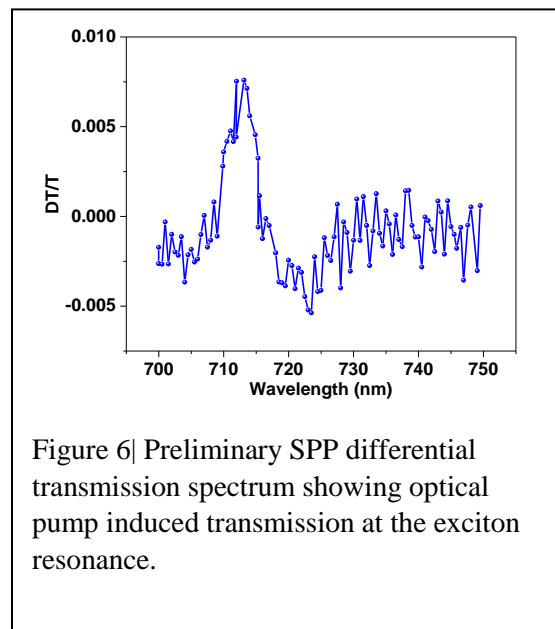


Figure 4| a) Optical microscope image of the plasmonic structure with an integrated hBN-WSe<sub>2</sub>-hBN heterostructure. Input and output couplers are labelled. The length of the plasmonic structure is 15 μm b) Optical microscope image of the focused laser exciting the input coupler (SPP Input) and light emission from the output coupler (SPP output). In the experiments, the output signal is isolated using spatial filtering.

data to the photoluminescence spectrum (Figure 5b), we can identify the dip in the SPP transmission as originating from the WSe<sub>2</sub> neutral exciton (X<sup>0</sup>).



The transmission spectrum of the plasmonic device can be controlled by optically pumping the excitons in the WSe<sub>2</sub> layer. In these experiments, transmission through the hBN-WSe<sub>2</sub>-hBN/plasmonic structure is measured while a 532 nm laser pumps the hBN-WSe<sub>2</sub>-hBN layer from above. Figure 6 shows a preliminary differential transmission spectrum normalized to the transmission through the plasmonic waveguide (DT/T). The peak at 712 nm in the differential transmission spectrum shows that the 532 nm pump laser saturates excitons in the WSe<sub>2</sub> layer, giving rise to an increase in SPP transmission. This optical pump-SPP probe measurement is the first step towards the primary objective of demonstrating SPP coherent wave-mixing in 2D material plasmonic structures.



*Fabrication of graphene devices for THz plasmonics*

In this project, THz SPPs bound to doped graphene monolayers were also investigated for applications to plasmonic amplification through coherent wave mixing. In year 1 of this project, hBN encapsulated graphene monolayers were fabricated (Figure 7), and preliminary characterization through transport and photocurrent were performed.

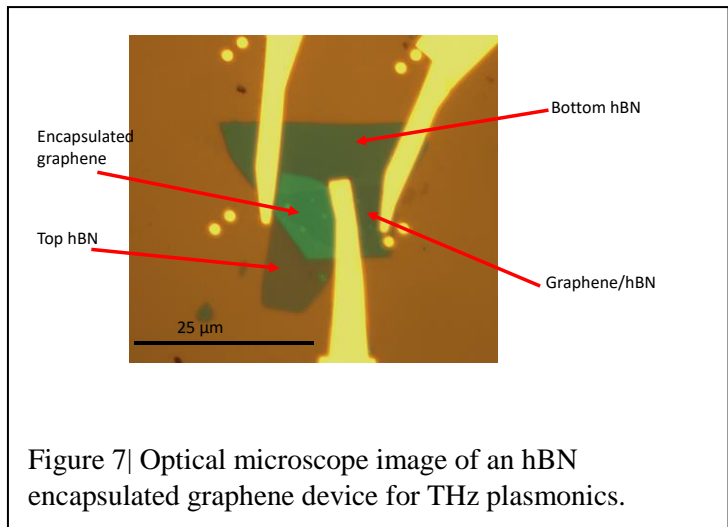


Figure 7| Optical microscope image of an hBN encapsulated graphene device for THz plasmonics.

**Year 2 Results:**

In year two of this project, we focused on developing 2D semiconductor plasmonic structures, which has resulted in the submission of the paper “2D Semiconductor Nonlinear Plasmonic Modulators” published in Nature Communications (2019). Due to the success of the 2D semiconductor plasmonic structures, we postponed the study of surface plasmons hosted in doped graphene and doped TMDs.

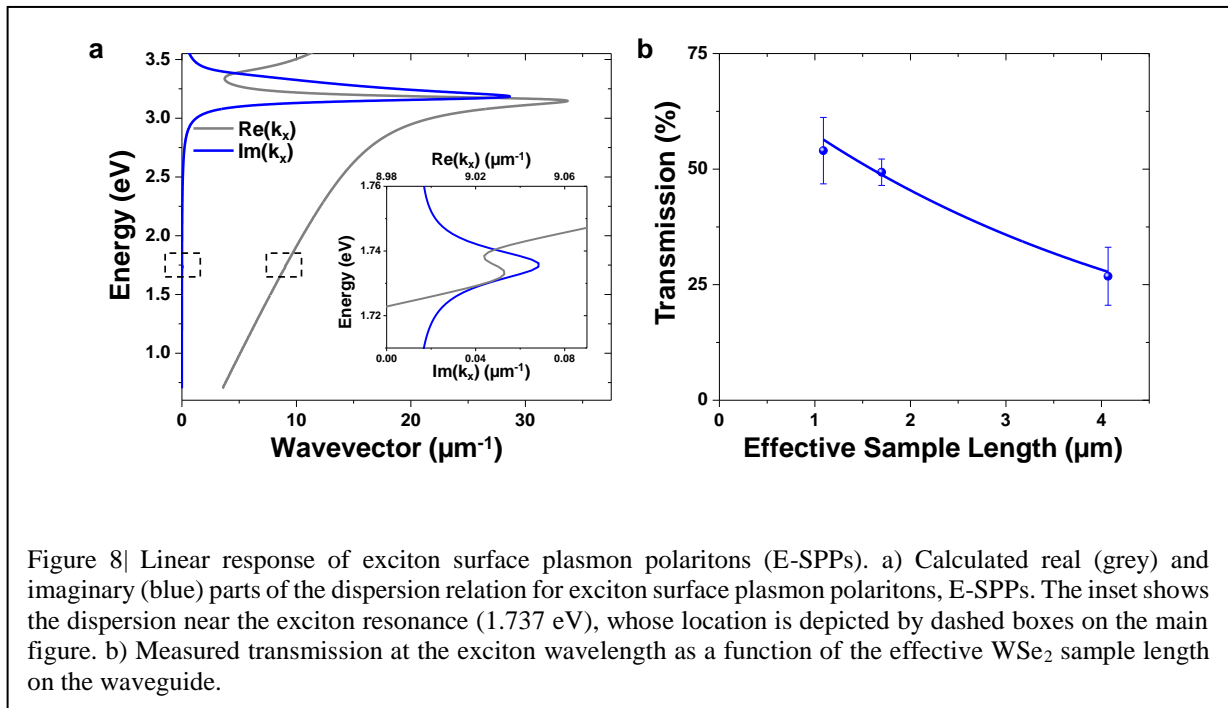


Figure 8| Linear response of exciton surface plasmon polaritons (E-SPPs). a) Calculated real (grey) and imaginary (blue) parts of the dispersion relation for exciton surface plasmon polaritons, E-SPPs. The inset shows the dispersion near the exciton resonance (1.737 eV), whose location is depicted by dashed boxes on the main figure. b) Measured transmission at the exciton wavelength as a function of the effective  $\text{WSe}_2$  sample length on the waveguide.

### Linear response of exciton surface plasmon polariton

Working with our theoretical collaborator Professor Rolf Binder (UA), we developed a theoretical model for the linear and nonlinear response of the 2D semiconductor integrated plasmonic structure. The dispersion of the exciton-SPP coupled system is shown in Figure 8a. The  $\text{Im}k_x$  of  $0.07 \mu\text{m}^{-1}$  corresponds to an absorption length of  $7.1 \mu\text{m}$ . Figure 8b shows the experimentally measured transmission for three different length samples. A fit to these data reveal an absorption length of  $4.2 \mu\text{m}$ , within a factor of two our theory.

### Resonant control of SPP propagation using optical and SPP pump

In order to demonstrate modulation of the SPP transmission, we performed two-color continuous wave pump-probe measurements. The experiment is depicted in Figure 9a where an optical pump laser is focused onto the WSe<sub>2</sub> monolayer while an SPP probe is coupled through the waveguide device. Figure 9b shows the DT/T spectra for the transmitted SPP probe as a function of three different pump wavelengths. The strongest resonance occurs when pump and probe are resonant with the neutral exciton at  $\sim 1.74$  eV (black curve). Here the positive DT response is consistent with saturating the exciton resonance, increasing the SPP probe transmission. Figure 9c shows the amplitude of the DT signal as function of optical pump power. The linear dependence of the DT response is consistent with a third-order nonlinear effect.

### Resonant control of SPP propagation using SPP pump

In order to demonstrate SPP controlled SPP propagation, we coupled both pump and probe lasers into the waveguide structure (depicted in Figure 10a) and repeat the frequency dependent pump probe measurements. The DT/T spectra are shown in Figure 10b for three different SPP pump energies. Again, we obtain the strongest DT response when both pump and probe are resonant with the neutral exciton near 1.74 eV. Remarkably the magnitude of the DT/T

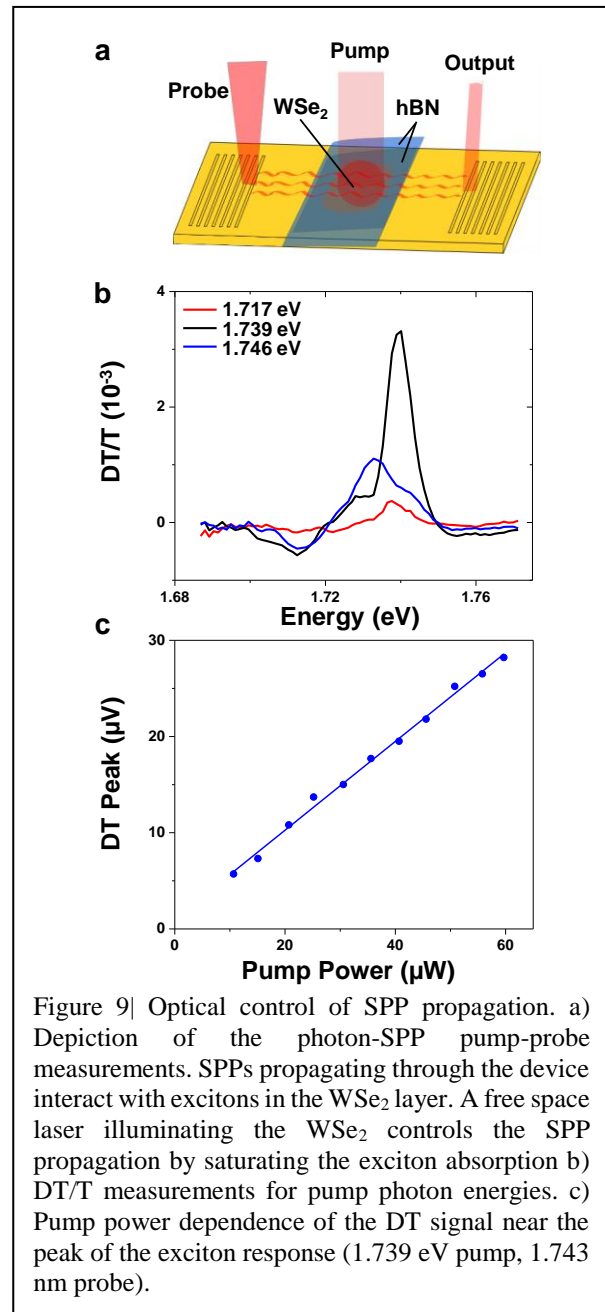


Figure 9| Optical control of SPP propagation. a) Depiction of the photon-SPP pump-probe measurements. SPPs propagating through the device interact with excitons in the WSe<sub>2</sub> layer. A free space laser illuminating the WSe<sub>2</sub> controls the SPP propagation by saturating the exciton absorption b) DT/T measurements for pump photon energies. c) Pump power dependence of the DT signal near the peak of the exciton response (1.739 eV pump, 1.743 nm probe).

response is approximately 4%, enhanced by an order of magnitude over the optical pumping case. In collaboration with Rolf Binder, we were able to determine that  $\text{Im}\chi^{(3)}$  to be  $-10^{-20} \frac{\text{m}^3}{\text{V}^2}$ , which is consistent with previously reported values of the third-order nonlinear susceptibility for  $\text{WSe}_2$ .

In addition to the steady state nonlinear spectroscopy measurements, we performed time resolved DT/T to probe the temporal response time, and demonstrated an ultrafast plasmonic modulation effect. We measured an ultrafast response time of  $\sim 290$  fs with a slower component of  $\sim 14$  ps (Fig. 11). The large DT/T response will be used in year three to demonstrate SPP four-wave-mixing and SPP amplification in the “cross waveguide” structures described below.

### *Development of cross waveguides for four-wave-mixing*

In order to realize four-wave-mixing in the phase conjugate geometry, we developed a cross-waveguide structures, which are depicted in Figure 11a. These waveguides have four different grating couplers allowing for the realization of counter-propagating pump waves (for example, by pumping the “upper” and “lower” gratings). The structure is composed of two  $5 \times 15 \mu\text{m}$  rectangular waveguides that cross at  $90^\circ$ . Figures 11b-f are Lumerical numerical simulations of the waveguide structure. They show the electric field mode profile as a function of height (Z) above the waveguide and (Y) across the middle region of the waveguide for various positions along the X direction which are labelled in Figure 11a. Figure 12a-b shows the calculated transmission of the waveguide structure. An important feature is that if the SPP is launched from the “input” coupler on the left side of the device  $>99\%$  of the SPP couples out through the output grating coupler. This directionality enabled the cross-propagating pump scheme that was used in year 3 to investigate plasmonic amplification.

### **Year 3 Results:**

In year 3, we focused on the fabrication and optical investigation of the “cross-waveguide” structures depicted in Figure 14. The devices have the potential to realize plasmonic amplification

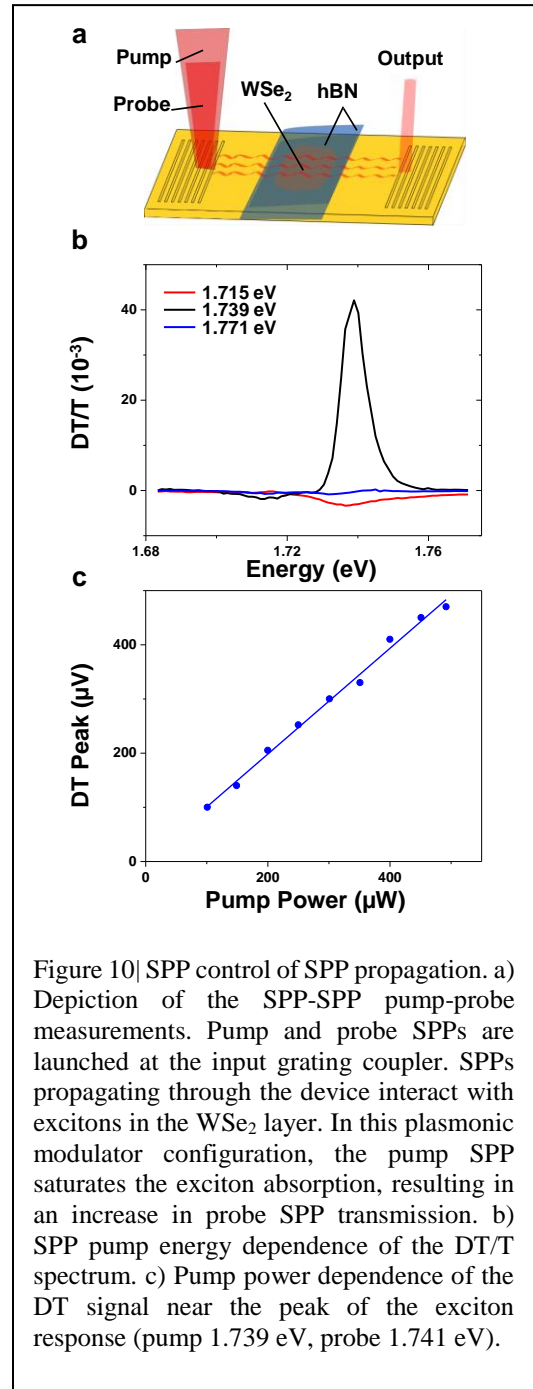
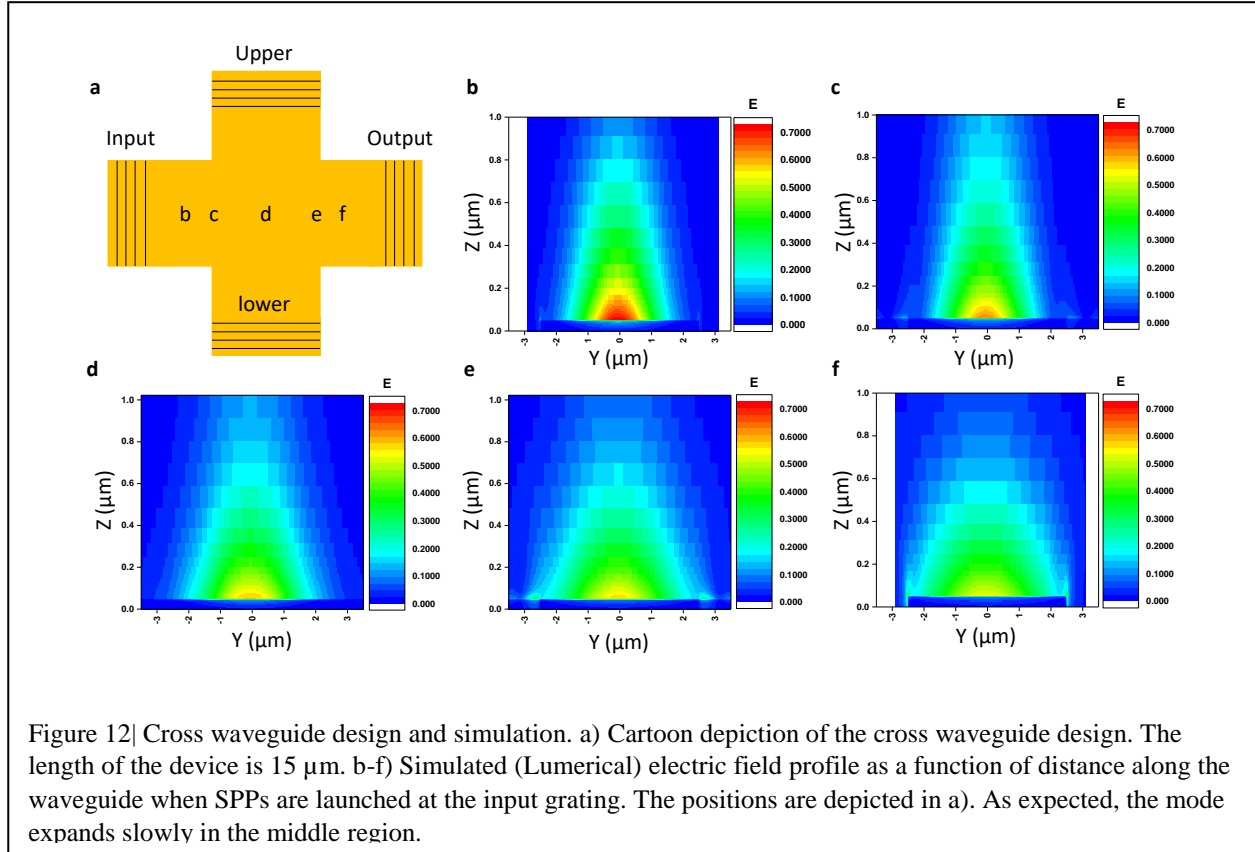
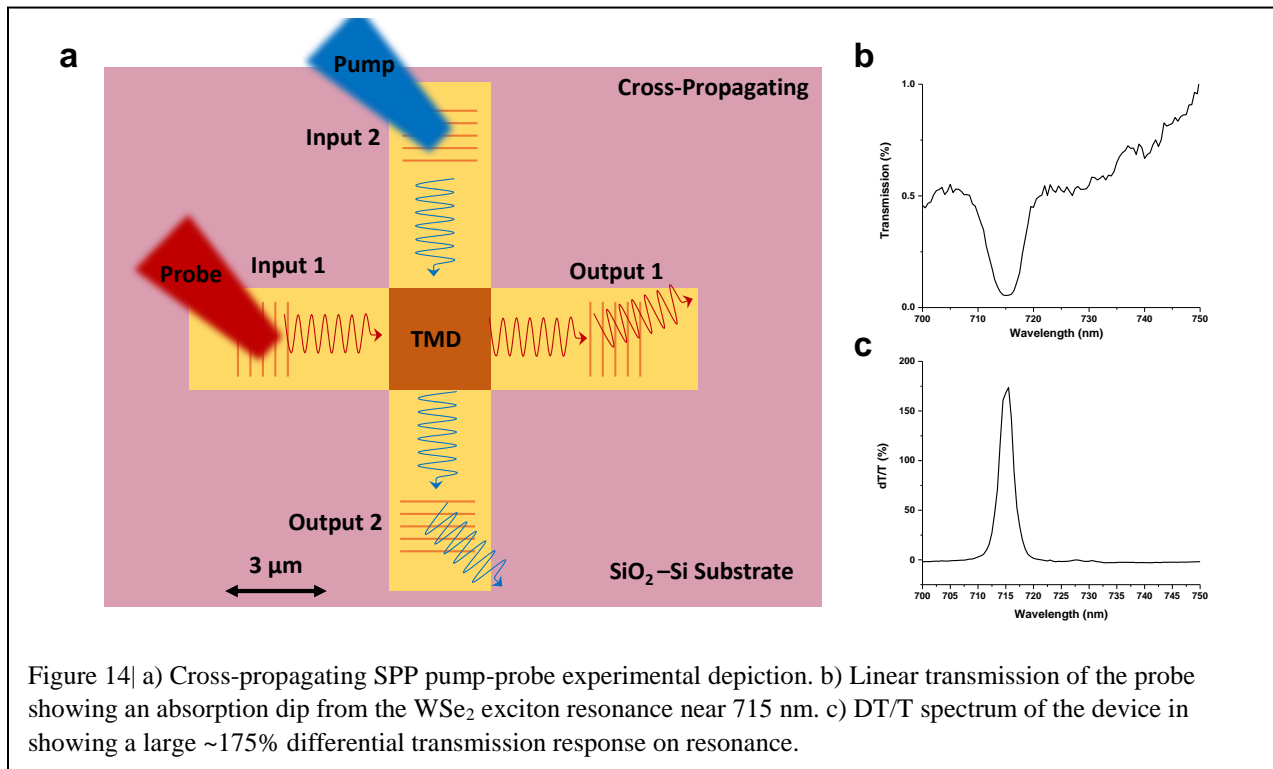
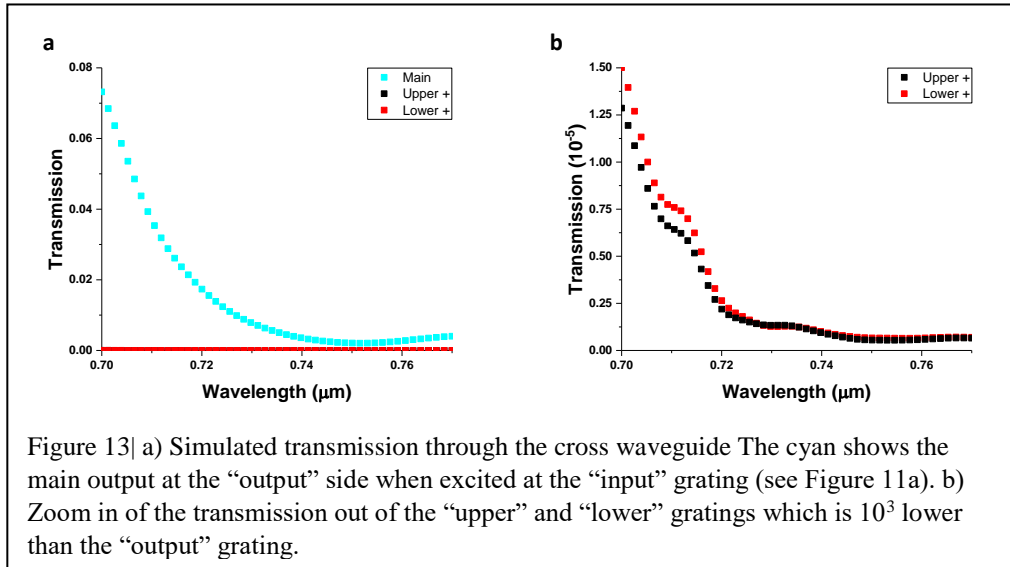


Figure 10| SPP control of SPP propagation. a) Depiction of the SPP-SPP pump-probe measurements. Pump and probe SPPs are launched at the input grating coupler. SPPs propagating through the device interact with excitons in the  $\text{WSe}_2$  layer. In this plasmonic modulator configuration, the pump SPP saturates the exciton absorption, resulting in an increase in probe SPP transmission. b) SPP pump energy dependence of the DT/T spectrum. c) Pump power dependence of the DT signal near the peak of the exciton response (pump 1.739 eV, probe 1.741 eV).

by scattering energy from the pump waves into the direction of the probe wave. We first fabricated bare cross-waveguide structures and characterized their transmission spectra which agreed well with the theoretical model. We then transferred hBN-encapsulated WSe<sub>2</sub> monolayer the middle of the cross structure as depicted in Figure 14a.



The measurements were performed at 5 K in an optical cryostat. The experimental configuration is depicted in Figure 14a. A pump SPP was launched by focusing a pump laser at Input 2 at the top of the device, and cross propagating probe SPP was launched by a probe laser focused at Input 1 on the left of the device. The linear probe transmission spectrum (Figure 14b), shows a pronounced dip at the WSe<sub>2</sub> exciton resonance similar to the rectangular waveguide structures (Figure 5a). The nonlinear DT/T response again shows a resonance at the same spectral position but its magnitude is approximately 44 times stronger than the co-propagating DT/T (Figure 10b) realizing an **exceptionally large resonant DT/T response of 175%**. This experiment was completed at the end of the project, and we currently preparing a manuscript on this topic. Specifically, we are working with our theoretical collaborator Rolf Binder to understand the extremely large magnitude of this nonlinear response, which we attribute to the proposed four-wave mixing amplification mechanism.



## Conclusion:

**In year 1** of this project, hybrid 2D material plasmonic structures have been designed, fabricated successfully. The coupling between SPPs and excitons in monolayer  $\text{WSe}_2$  have been demonstrated, and all optical control of SPP have been demonstrated. **In year 2**, we demonstrated optical and SPP controlled modulation of SPP propagation, developed a model for exciton-SPP coupling and were able to extract quantitative values for the third order nonlinear susceptibility. We also designed and modelled the cross waveguides that will be used in the four-wave mixing

measurements, and have fabricated preliminary cross waveguide structures that will also enable electrical control of the TMD doping level. **In year 3**, coherent wave-mixing between SPPs were be explored, specifically in the context of four-wave-mixing effects that give rise to amplification. We are currently preparing a manuscript on the cross-propagating experiments described above. Our future projects will focus on further enhancing the nonlinear response using heterostructures and adding tuning dielectric layers to increase the SPP-exciton interaction.